Formic Acid Photoreforming for Hydrogen Production on Shape-Controlled Anatase TiO2 Nanoparticles: Assessment of the Role of Fluorides, 101/001 Surfaces Ratio, and Platinization

Formic Acid Photoreforming for Hydrogen Production on Shape-Controlled Anatase TiO_2 Nanoparticles: Assessment of the Role of Fluorides, {101}/{001} Surfaces Ratio and Platinization

Francesco Pellegrino[a*], Fabrizio Sordello[a], Lorenzo Mino[a], Claudio Minero[a], Vasile-Dan Hodoroaba[b], Gianmario Martra[a], Valter Maurino[a*]

a) Dipartimento di Chimica and NIS Inter-departmental Centre, University of Torino, Via P. Giuria 7, Torino, 10125, Italy

b) Federal Institute for Materials Research and Testing (BAM), 12205 Berlin, Germany

ABSTRACT: Hydrogen production via formate photoreforming on TiO_2 is characterized by marked dependence on the ratio between {101} and {001} surfaces for anatase nanoparticles. We observed higher rates of hydrogen evolution with the increase of the {101} facets presence, owing to their reductive nature. This helps the Pt photo-deposition in the early stages of irradiation, and then the hydrogen ion reduction reaction. The selective photo-deposition of 2 nm Pt nanoparticles on {101} facets was confirmed by TEM micrographs. The results are confirmed also by experiments carried out without the use of Pt as co-catalyst and by photoelectrochemical measurements. The work also explains the marginal effect of the fluorination on the H_2 evolution.

KEYWORDS. Titanium Dioxide; Fluoride; Platinum; Controlled Shape; Hydrogen photoproduction; Surface; Photoreforming

INTRODUCTION

The conversion of solar energy into electricity and high added value chemicals is of paramount importance for a sustainable future[1]. However, many challenges remain in order to exploit solar energy[2]. The feasibility of photo-electrochemical water splitting was demonstrated long ago,[3] but H_2 photoproduction efficiencies are still low[4], and improvements for photo-electrochemical cells for water splitting[5], organics reforming[6] and artificial photosynthesis[7] are actively pursued. The optimization of these systems requires a deep understanding of the phenomena and reaction mechanisms involved at molecular level.

In this respect, TiO_2 is a key photoactive material, and in the last decades several works have been devoted to the modification and control of the TiO_2 structure[8], particle size and morphology[9], to maximize photogenerated charge carrier separation and interfacial charge transfer.[6c, 6d, 10] Surface properties at molecular level, crystal faceting and reconstruction have revealed as key feature in controlling interfacial charge transfer in anatase nanoparticles.[11] Surface states of the anatase {101} surface seem to favor semiconductor to electrolyte electron transfer, e.g. cathodic processes, leading to faster H_2 photoproduction.[9b, 10d, 12] Conversely, the {001} facets were proposed to be the location of photo-induced anodic processes (e.g. oxygen evolution reaction, OER) [10a]. However, the reported results are somewhat contradictory, probably due to different surface terminations/reconstruction depending on the synthesis condition and post synthetic treatments of the anatase nanoparticle.[13] Hydrogen Evolution Reaction (HER) on TiO_2 can be studied following two approaches: the first provides the use of a co-catalyst - usually a noble

metal - for improving the activity of the nanoparticles obtaining higher H_2 amounts, the second, instead, studies the bare nanoparticles for understanding the peculiar reactivity of the unaffected TiO_2 facets.[14] Several works have deeply investigated the effect of different co-catalysts - and of their amount - as well as the role of exposed surface and morphology of TiO_2 nanoparticles, both in the HER and the wastewater remediation.[9b, 10b, 14-15]

In 2011, Yi and coworkers[16] investigated the role of the TiO_2 nanoparticles shape in the photocatalytic hydrogen evolution. They compared nano-spheres and nanorods using Pt as co-catalyst (1 wt %) and ethanol as sacrificial agent. They found that TiO_2 nanorods have higher photocatalytic activity due to a decreased probability of e^-/h^+ recombination. The authors, however, did not investigate the role of different surfaces present in their materials, probably responsible for different electron-hole recombination rates. More recent works carried out by D'Arienzo et al. in 2015[10a] and Liu et al. in 2017,[10b] suggested the presence of a "surface heterojunction" between {101}, {010} and {001} facets, which favors the charge separation for nanoparticles with an intermediate amounts of the oxidative and reductive surfaces. Different electrochemical potential of electrons on {101} and {001} facets favors the charge carrier separation, acting as a junction with an associate potential drop. Conversely, in 2012 Gordon et al. found that bipyramidal nanoparticles that largely expose {101} facets present higher hydrogen evolution rate due to the reductive nature of these surfaces.[9b] While in the former cases H_2 photo-production was carried out on pristine TiO_2, in the absence of any co-catalyst, Gordon et al. employed Pt-loaded TiO_2 NPs. Therefore, the different behavior reported by different authors could be due to platinization.

To shed light on this ambiguity, here we investigated formic acid photoreforming (formally: $HCOOH \rightarrow H_2 + CO_2$) on shape-controlled TiO_2 NPs with different – and controlled – {101}:{001} surface ratios, both in the presence and in the absence of Pt as co-catalyst.[14, 17] Moreover, TiO_2 nano-sheets are typically obtained using F^- as templating agents, which remain in significant amount both in the bulk and at the surface of these nanoparticles.[13b, 18]

Due to the different redox behavior of anatase TiO_2 facets, HCOOH oxidation is expected to preferentially occur at the {001} facets, while Pt deposition and HER predominantly take place on the {101} facets[12].

In the absence of Pt, the H_2O reduction to H_2 is a slow process, so electrons are less rapidly scavenged and they are prone to recombination with the photogenerated holes. Therefore, it can be proposed that HER is limiting the rate of the photocatalytic HCOOH reforming, at least in the absence of Pt.

To gain further insight, for the first time H_2 evolution was also described from an electrochemical point of view by means of open circuit potential (OCP) and cyclic voltammetry (CV). Furthermore, the effect of bulk and surface fluorination was considered.

RESULTS AND DISCUSSION

Table 1 summarizes the main morphological characteristics of the four considered materials, as determined in a previous work.[13b] Particle sizes of all the materials considered are similar. The only material that differs are the bipyramidal nanoparticles, which have a width (a-axis) of 35 (±5) nm, compared to 75 (±25) nm of the nanosheets (n-sh). The thickness (c-axis) of bipyramids and nanosheets are 45 nm and 10 nm respectively, reflecting the different morphology of the two materials. However, surface area and volumes of these NPs are very similar. Representative HR-SEM images are show in Figure 1. The sample n-sh is composed of anatase nanosheets, synthesized in the presence of fluorides as shape controllers and, therefore, mainly expose {001} facets (80%) and only 20% of {101} surfaces. Noteworthy, F^- were found both in the bulk and at surfaces (see SI and ref. 12b).

Table 1. Main morphological characteristics of the four considered materials.[13b]

Material	Thickness, nm c-axis	Width, nm a and b-axis	SSA_{BET}, $m^2 g^{-1}$	% {101}	{101}:{001} Ratio	Phase
n-sh	9.4 ± 1.6	75 ± 25	53	22	~ 0.3	Anatase
n-sh_NaOH	8.4 ± 1.7	73 ± 23	57	21	~ 0.3	Anatase
n-sh_873K	10 ± 2	64 ± 25	34	42	~ 0.7	Anatase
bipy_873K	45 ± 9	35 ± 5	37	90	~ 9.0	Anatase

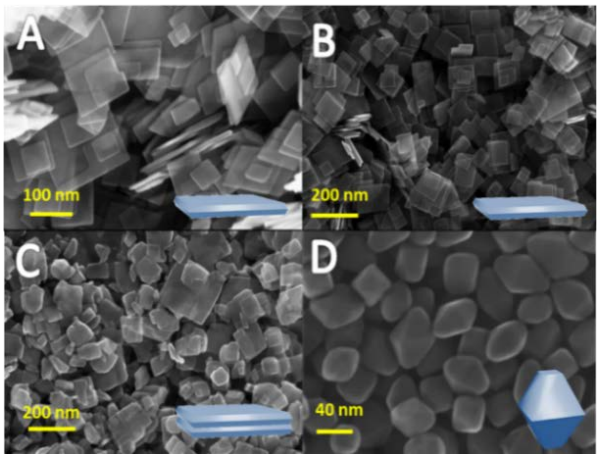

Figure 1. SEM micrographs of the 4 four materials considered: A) n-sh; B) n-sh_NaOH; C) n-sh_873K D) bipy_873K..Scale bars: A and B) 20 nm; C and D) 100 nm

The sample n-sh_NaOH derives from n-sh, by substitution of surface F^- with OH^-. Nevertheless, the morphology does not change compared with n-sh, and then the sample n-sh_NaOH still exposes 20% of {101} facets. The sample n-sh_873K is obtained from sample n-sh by calcination at 873 K, which induces a (1x4) reconstruction of {001} surface (see SI) and an almost complete removal of F^-. The fluorides content in the three kinds of nanosheets nanoparticles is reported in the SI. Previous investigations revealed that a sintering between pair of platelets occurred through their basal {001} facets, and, therefore, an increase in the relative abundance of the {101} surfaces, corresponding now to 40% of the exposed terminations. The last sample, bipy_873K, is made of truncated bipyramids, prepared in the absence of F^-, mainly exposing {101} surfaces (90%). Details on the preparation and characterization are in SI and ref [13b].

For all materials, platinization was carried out by photoreduction of H_2PtCl_6 (further information in SI). The amount of deposited Pt was of ca. 0.2 wt%, in form of nanoparticles 2-3 nm in size (Figure 2; additional images and size distribution in Supporting Information).

By controlling the shape of the TiO_2 NPs, it is possible to confine Pt nanoparticles in limited regions, as it is the case of TiO_2 nanosheets, where Pt deposition mainly occurs at the sheet {101} edges, being the reductive surface.[12] Conversely, in the case of bipyramids, which mainly expose the reducing {101} facets, Pt nanoparticles are widespread across the whole particles.

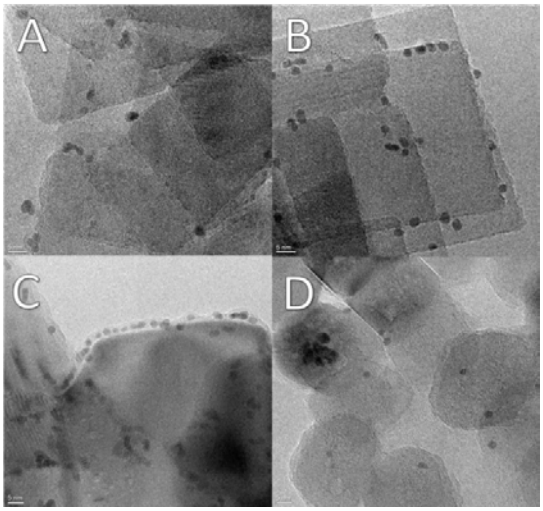

Figure 2. TEM micrographs of the Pt nanoparticles deposited on n-sh (A), n-sh_NaOH (B), n-sh_873K (C) and bipy_873K (D). Scale bar: 5 nm in all the panels.

For all materials, a constant H_2 photoproduction vs time was observed (and consequently also for CO_2, Figure 3 and Figure S5). The obtained values are listed in Table 2.

Table 2. Photocatalytic H_2 evolution rate, normalized with respect to the total surface area, from the four considered materials in the presence and in the absence of Pt as co-catalyst under irradiation of 15 W m^{-2} centered at 365 nm.

	Bare TiO_2	**Pt/TiO_2**
Material	**Rate, mmol H_2 m^{-2} TiO_2 min^{-1}**	**Rate, mmol H_2 m^{-2} TiO_2 min^{-1}**
n-sh	$(2.5\pm0.8)\times10^{-6}$	$(2.9\pm0.1)\times10^{-4}$
n-sh_NaOH	$(1.4\pm0.8)\times10^{-6}$	$(2.9\pm0.1)\times10^{-4}$
n-sh_873K	$(1.6\pm0.1)\times10^{-5}$	$(7.0\pm0.3)\times10^{-4}$
bipy_873K	$(3.0\pm0.2)\times10^{-5}$	$(1.8\pm0.1)\times10^{-3}$

Focusing on bare TiO_2 nanoparticles, no differences within the uncertainty range of the measurements were obtained for n-sh and n-sh_NaOH, indicating that the substitution of surface F^- with OH^- has negligible impact on the H_2 production. This is not obvious since it is well known that the presence of F^- ions can strongly impact the surface properties of the nanoparticles, altering the adsorption energy, the diffusion length of charge carriers, etc.[19] The reason for such a small influence can be ascribed to the low coverage of the fluorides on the {101} facets, which are mainly involved in the H_2 production and Pt photodeposition. Indeed, fluorides are used as shape controllers for obtaining {001} surfaces, so the majority of the F^- present in the n-sh material are bound to these facets, which are marginally involved in the photocatalytic H_2 evolution. However, they can affect the formic acid degradation, hindering the surface of the nanoparticles and reducing the photocatalytic oxidation of this substrate[20]. Nevertheless, because the overall rate is limited by the reduction semi-reaction, the effect is negligible. Conversely, F^- free n-sh_873K showed a H_2 photoproduction rate at least 5 times larger. As reported above, the obtained removal of fluorides from both bulk and surfaces was accompanied by a doubling of the relative amount of exposed {101} terminations. Thus, the obtained increase in the H_2 photoproduction rate cannot be related to a change of only one feature of the nanoparticles. Finally, a further increase of ca. 2 times of H_2 photoproduction rate was measured for bipy_873K, limited by an almost double relative amount of {101} facets.

Platinization improved significantly the H_2 photoproduction rate of all samples, with a gain of ca. 2 orders of magnitude for n-sh and n-sh_NaOH, whilst for n-sh_873K and bipy_873K was limited to 50-60 times. The importance of the Pt role is also confirmed by the CO_2 evolution rates. In fact, in the presence of Pt the ratio between the CO_2 production and H_2 production is near 1 (though slightly in favor of CO_2, Figure 3). Whereas in the absence of Pt the rate of CO_2 production is significantly higher compared to the H_2 production (Figure S5). This could be ascribed to the presence of residual O_2 (constantly monitored and always lower than 0.04%) that, acting as electrons scavenger, can decouple H_2 production from CO_2 evolution without Pt, pointing out the crucial role of the co-catalyst in HER.

This results confirm the increase of the H_2 production rates with the increase of the {101} percentage in the materials for both bare and platinized TiO_2 nanoparticles. Indeed, the highest rate is obtained for the bipy_873K, with a ca. 90% of {101} terminations. Whereupon, among nanosheets NPs, the calcined sample has the highest photoactivity and the largest amount of {101} surfaces, and n-sh and n-sh_NaOH, that have nearly the same amount of {101} surface, show almost the same photocatalytic H_2 evolution rate.

In order to evaluate the possible effect of additional factors with respect to the relative amount of exposed {101} surfaces, the H_2 evolution rates were normalized for the fraction of specific surface area due only to {101} (i.e total SSA_{BET} times the % of {101}). The results are shown in Figure 4, highlighting the presence of a maximum in the trend obtained for bare TiO_2 nanoparticles, corresponding

to the n-sh_873K, which exposes nearly the same amount of {101} and {001} facets.

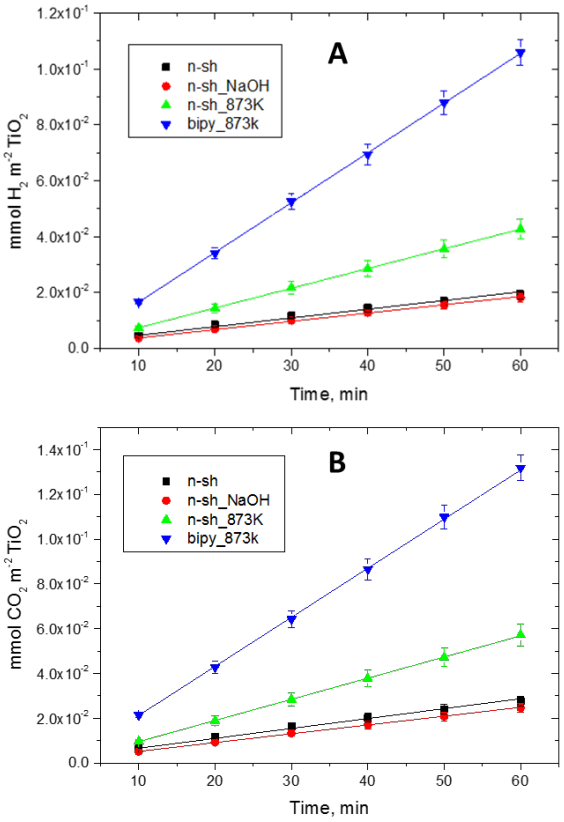

Figure 3. Photocatalytic H_2 (A) and CO_2 (B) production curves obtained at pH 3.5 for the studied materials in presence of Pt as co-catalyst.

This seems in agreement with the possible role of "surface heterojunction".[10a, 10b, 14, 21] Conversely, the same trend already observed in Table 2 was obtained for platinized TiO_2 nanoparticles. This behavior could be ascribed to the higher density of Pt nanoparticles on the {101} surface of the nanosheets (see Supporting Information, Table S2). Such high density might play a detrimental role because in this case metal nanoparticles could act as recombination centers, as already observed for high loading of metal nanoparticles deposited on TiO_2.[15b, 22]

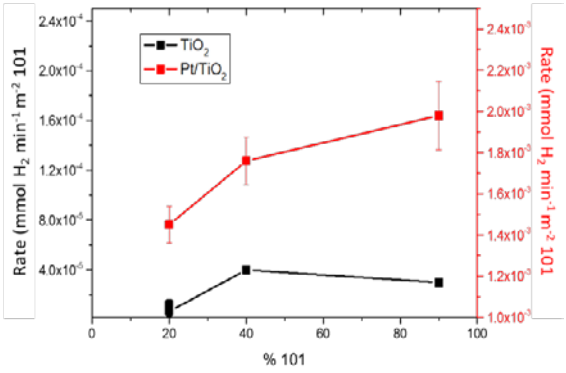

Figure 4. Photocatalytic H_2 production rates normalized for the {101} specific surface area only as functions of the {101}:{001} ratio in the presence (red) and in the absence (black) of Pt.

Electrochemical measurements were carried out on the different TiO_2 deposited on ITO electrodes to evaluate the rate of photoelectron transfer to solution. For this purpose, we applied the method developed by Gomez[23]. This combines CVs in the dark and OCP relaxation tests (Figure 5 and Figures S7-S8). Details on this data treatment are in SI. In this way, it is possible to obtain the density of charge carriers generated and their recombination or transfer rate.

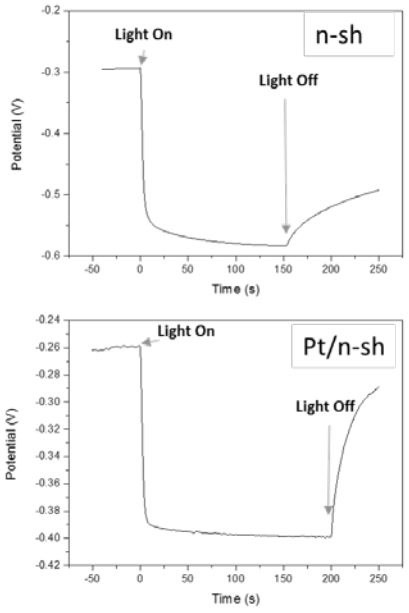

Figure 5. OCP measurements carried out on the TiO_2 electrodes prepared starting from the material n-sh in the absence (top) and in the presence (bottom) of Pt as co-catalyst. N_2 atmosphere. pH 3.7, formate buffer 0.1 M.

Several characteristics (morphology, platinization, and fluorination) of the TiO_2 nanoparticles can influence the charge transfer rate. Figure 6 reports the photoelectron decay rate constant (k_d) of the considered materials in the presence and in the absence of Pt as co-catalyst.

Electrochemical measurements show that photogenerated electron decay increases up to four times upon platinization. The increase of the steady state H_2 photoproduction rate on Pt/TiO_2 means that the faster photoelectron decay is due to their increased transfer to solution species, namely H^+ (fast reaction, but limited by proton concentration) and water (slower reaction, but very large concentration > 55 M).

The photoelectrochemical measurements are coherent with the H_2 evolution trends obtained during formic acid photoreforming. Indeed, the higher is the amount of the {101} surface on the material, the higher is k_d (again with a saturating trend). This clearly indicates the crucial role of the {101} surface as cathodic site for H_2 evolution.

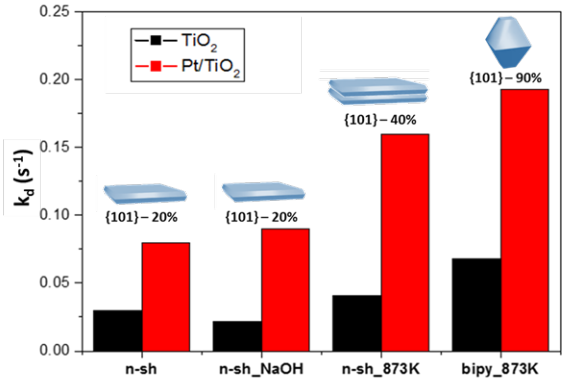

Figure 6. Initial rate constant for electron transfer (k_d) of the considered materials in the presence and in the absence of Pt as co-catalyst.

CONCLUSIONS

The work presents the study of the H_2 production from formate buffer photoreforming using four shape controlled TiO_2 anatase nanoparticles with and without Pt as co-catalyst under UV irradiation. The results highlight the importance of the TiO_2 particle shape on H_2 evolution, and confirm the increase of the H_2 production rates with the increase of the {101} surfaces amount in the material, due to the reducing character of this facet. A deeper investigation of the surface {101} reactivity highlights that, in the absence of a co-catalyst, an optimal ratio between {101} and {001} surface occurs when the two facets are present in a similar amount, confirming the presence of a "surface heterojunction" that increase the reactivity of the {101} surface. Pt as co-catalyst partially limits this maximum of reactivity, giving a saturative trend of the reactivity (see Figure 4), thanks to the increased rate of electrons transfer. TEM micrographs show that 2-3 nm Pt nanoparticles are almost selectively deposited on the {101} surfaces. The effect of superficial fluorination for this type of samples remains, instead, marginal. Finally, photoelectrochemical experiments clearly confirmed the high impact of the TiO_2 nanoparticles morphology on the charge carriers' transfer rate. Therefore, we demonstrated that tuning the shape of TiO_2 NPs and modulating the ratio between the surfaces {101} and {001} allows the improvement of the photocatalytic hydrogen production.

ASSOCIATED CONTENT

Supporting Information includes data about the synthesis and characterization of the nanoparticles, experimental set-up for hydrogen detection and supplementary photoelectrochemical tests.

AUTHOR INFORMATION

Corresponding Authors

*E-mail: francesco.pellegrino@unito.it
valter.maurino@unito.it

Author Contributions

The manuscript was written through contributions of all authors. All authors have given approval to the final version of the manuscript.

Funding Sources

The authors acknowledge funding from SETNanoMetro, EU Project, FP7-NMP-2013_LARGE-7. Project number: 604577

REFERENCES

1. Armaroli, N.; Balzani, V., The Future of Energy Supply: Challenges and Opportunities. *Angewandte Chemie* **2007,** *46* , 52-66.
2. (a) Tributsch, H.; Neumann, B., Material Research Challenges Towards a Corrosion Stable Photovoltaic Hydrogen-

Generating Membrane. *Int J Hydrogen Energ* **2007,** *32*, 2679-2688; (b) Tributsch, H., Photovoltaic Hydrogen Generation. *Int J Hydrogen Energ* **2008,** *33*, 5911-5930.
3. (a) Reece, S. Y.; Hamel, J. A.; Sung, K.; Jarvi, T. D.; Esswein, A. J.; Pijpers, J. J. H.; Nocera, D. G., Wireless Solar Water Splitting Using Silicon-Based Semiconductors and Earth-Abundant Catalysts. *Science* **2011,** *334*, 645-648; (b) Osterloh, F. E., Inorganic Nanostructures for Photoelectrochemical and Photocatalytic Water Splitting. *Chemical Society reviews* **2013,** *42*, 2294-2320.
4. Peharz, G.; Dimroth, F.; Wittstadt, U., Solar Hydrogen Production by Water Splitting with a Conversion Efficiency of 18%. *Int J Hydrogen Energ* **2007,** *32*, 3248-3252.
5. Zhou, Y.; Huang, Y.; Li, D.; He, W. H., Three-Dimensional Sea-Urchin-like Hierarchical TiO_2 Microspheres Synthesized by a One-Pot Hydrothermal Method and their Enhanced Photocatalytic Activity. *Mater Res Bull* **2013,** *48*, 2420-2425.
6. (a) Chiarello, G. L.; Dozzi, M. V.; Scavini, M.; Grunwaldt, J. D.; Selli, E., One Step Flame-Made Fluorinated Pt/TiO_2 Photocatalysts for Hydrogen Production. *Appl Catal B-Environ* **2014,** *160*, 144-151; (b) Lee, K.; Hahn, R.; Altomare, M.; Selli, E.; Schmuki, P., Intrinsic Au Decoration of Growing TiO_2 Nanotubes and Formation of a High-Efficiency Photocatalyst for H_2 Production. *Advanced materials* **2013,** *25*, 6133-6137; (c) Priebe, J. B.; Radnik, J.; Lennox, A. J. J.; Pohl, M.-M.; Karnahl, M.; Hollmann, D.; Grabow, K.; Bentrup, U.; Junge, H.; Beller, M.; Brückner, A., Solar Hydrogen Production by Plasmonic Au–TiO_2 Catalysts: Impact of Synthesis Protocol and TiO_2 Phase on Charge Transfer Efficiency and H_2 Evolution Rates. *ACS Catalysis* **2015,** *5*, 2137-2148; (d) Yuan, Y.-J.; Ye, Z.-J.; Lu, H.-W.; Hu, B.; Li, Y.-H.; Chen, D.-Q.; Zhong, J.-S.; Yu, Z.-T.; Zou, Z.-G., Constructing Anatase TiO_2 Nanosheets with Exposed (001) Facets/Layered MoS_2 Two-Dimensional Nanojunctions for Enhanced Solar Hydrogen Generation. *ACS Catalysis* **2015,** *6*, 532-541.
7. Roy, S. C.; Varghese, O. K.; Paulose, M.; Grimes, C. A., Toward Solar Fuels: Photocatalytic Conversion of Carbon Dioxide to Hydrocarbons. *ACS nano* **2010,** *4*, 1259-1278
8. Nikitenko, S. I.; Chave, T.; Cau, C.; Brau, H.-P.; Flaud, V., Photothermal Hydrogen Production Using Noble-Metal-Free Ti@TiO_2 Core–Shell Nanoparticles under Visible–NIR Light Irradiation. *ACS Catalysis* **2015,** *5*, 4790-4795.
9. (a) Chiarello, G. L.; Zuliani, A.; Ceresoli, D.; Martinazzo, R.; Selli, E., Exploiting the Photonic Crystal Properties of TiO_2 Nanotube Arrays To Enhance Photocatalytic Hydrogen Production. *ACS Catalysis* **2016,** *6*, 1345-1353; (b) Gordon, T. R.; Cargnello, M.; Paik, T.; Mangolini, F.; Weber, R. T.; Fornasiero, P.; Murray, C. B., Nonaqueous Synthesis of TiO_2 Nanocrystals Using TiF_4 to Engineer Morphology, Oxygen Vacancy Concentration, and Photocatalytic Activity. *J Am Chem Soc* **2012,** *134*, 6751-6761.
10. (a) D'Arienzo, M.; Dozzi, M. V.; Redaelli, M.; Di Credico, B.; Morazzoni, F.; Scotti, R.; Polizzi, S., Crystal Surfaces and Fate of Photogenerated Defects in Shape-Controlled Anatase Nanocrystals: Drawing Useful Relations to Improve the H_2 Yield in Methanol Photosteam Reforming. *J Phys Chem C* **2015,** *119*, 12385-12393; (b) Liu, J.; Olds, D.; Peng, R.; Yu, L.; Foo, G. S.; Qian, S.; Keum, J.; Guiton, B. S.; Wu, Z. L.; Page, K., Quantitative Analysis of the Morphology of {101} and {001} Faceted Anatase TiO_2 Nanocrystals and Its Implication on Photocatalytic Activity. *Chem Mater* **2017,** *29*, 5591-5604; (c) Tanaka, A.; Sakaguchi, S.; Hashimoto, K.; Kominami, H., Preparation of Au/TiO_2 with Metal Cocatalysts Exhibiting Strong Surface Plasmon Resonance Effective for Photoinduced Hydrogen Formation under Irradiation of Visible Light. *ACS Catalysis* **2012,** *3*, 79-85; (d) Belhadj, H.; Hamid, S.; Robertson, P. K. J.; Bahnemann, D. W., Mechanisms of Simultaneous Hydrogen Production and Formaldehyde Oxidation in H_2O and D_2O over Platinized TiO_2. *Acs Catalysis* **2017,** *7*, 4753-4758.
11. (a) Deiana, C.; Minella, M.; Tabacchi, G.; Maurino, V.; Fois, E.; Martra, G., Shape-Controlled TiO_2 Nanoparticles and TiO_2 P25 Interacting with CO and H_2O_2 Molecular Probes: a Synergic Approach for Surface Structure Recognition and Physico-Chemical Understanding. *Physical chemistry chemical physics : PCCP* **2013,** *15*, 307-315; (b) Minero, C.; Mariella, G.; Maurino, V.; Pelizzetti, E., Photocatalytic Transformation of Organic Compounds in the Presence of Inorganic Anions. 1. Hydroxyl-Mediated and Direct Electron-Transfer Reactions of Phenol on a Titanium Dioxide−Fluoride System. *Langmuir* **2000,** *16*, 2632-2641; (c) Günnemann, C.; Haisch, C.; Fleisch, M.; Schneider, J.; Emeline, A. V.; Bahnemann, D. W., Insights into Different Photocatalytic Oxidation Activities of Anatase, Brookite, and Rutile Single-Crystal Facets. *ACS Catalysis* **2018,** *9*, 1001-1012.
12. Taguchi, T.; Saito, Y.; Sarukawa, K.; Ohno, T.; Matsumura, M., Formation of New Crystal Faces on TiO_2 Particles by Treatment with Aqueous HF Solution or Hot Sulfuric Acid. *New J Chem* **2003,** *27*, 1304-1306.
13. (a) Selcuk, S.; Selloni, A., Surface Structure and Reactivity of Anatase TiO_2 Crystals with Dominant {001} Facets. *J Phys Chem C* **2013,** *117*, 6358-6362; (b) Mino, L.; Pellegrino, F.; Rades, S.; Radnik, J.; Hodoroaba, V.-D.; Spoto, G.; Maurino, V.; Martra, G., Beyond Shape Engineering of TiO_2 Nanoparticles: Post-Synthesis Treatment Dependence of Surface Hydration, Hydroxylation, Lewis Acidity and Photocatalytic Activity of TiO_2 Anatase Nanoparticles with Dominant {001} or {101} Facets. *ACS Applied Nano Materials* **2018,** *1*, 5355-5365.
14. Pellegrino, F.; Sordello, F.; Minella, M.; Minero, C.; Maurino, V., The Role of Surface Texture on the Photocatalytic H_2 Production on TiO_2. *Catalysts* **2019,** *9*, 32-59.
15. (a) Han, F.; Kambala, V. S. R.; Srinivasan, M.; Rajarathnam, D.; Naidu, R., Tailored Titanium Dioxide Photocatalysts for the Degradation of Organic Dyes in Wastewater Treatment: A Review. *Appl Catal a-Gen* **2009,** *359*, 25-40; (b) Sung-Suh, H. M.; Choi, J. R.; Hah, H. J.; Koo, S. M.; Bae, Y. C., Comparison of Ag Deposition Effects on the Photocatalytic Activity of Nanoparticulate TiO_2 under Visible and UV Light Irradiation. *J Photoch Photobio A* **2004,** *163*, 37-44.
16. Yun, H. J.; Lee, H.; Jool, J. B.; Kim, N. D.; Yi, J., Effect of TiO_2 Nanoparticle Shape on Hydrogen Evolution via Water Splitting. *Journal of nanoscience and nanotechnology* **2011,** *11*, 1688-1691.
17. (a) Lanese, V.; Spasiano, D.; Marotta, R.; Di Somma, I.; Lisi, L.; Cimino, S.; Andreozzi, R., Hydrogen Production by Photoreforming of Formic Acid in Aqueous Copper/TiO_2 Suspensions under UV-Simulated Solar Radiation at Room Temperature. *Int J Hydrogen Energ* **2013,** *38*, 9644-9654; (b) Chen, T.; Wu, G.; Feng, Z.; Hu, G.; Su, W.; Ying, P.; Li, C., In Situ FT-IR Study of Photocatalytic Decomposition of Formic Acid to Hydrogen on Pt/TiO_2 Catalyst. *Chinese Journal of Catalysis* **2008,** *29*, 105-107.
18. Ong, W. J.; Tan, L. L.; Chai, S. P.; Yong, S. T.; Mohamed, A. R., Highly Reactive {001} Facets of TiO_2-Based Composites: Synthesis, Formation Mechanism and Characterization. *Nanoscale* **2014,** *6*, 1946-2008.
19. (a) Tada, K.; Koga, H.; Hayashi, A.; Kondo, Y.; Kawakami, T.; Yamanaka, S.; Okumura, M., Effects of Halogens on Interactions between a Reduced TiO_2 (110) Surface and Noble Metal Atoms: A DFT Study. *Applied Surface Science* **2017,** *411*, 149-162; (b) Lamiel-Garcia, O.; Tosoni, S.; Illas, F., Relative Stability of F-Covered TiO_2 Anatase (101) and (001) Surfaces from Periodic DFT Calculations and Ab Initio Atomistic Thermodynamics. *The Journal of Physical Chemistry C* **2014,** *118*, 13667-13673.
20. Monllor-Satoca, D.; Lana-Villarreal, T.; Gomez, R., Effect of Surface Fluorination on the Electrochemical and Photoelectrocatalytic Properties of Nanoporous Titanium Dioxide Electrodes. *Langmuir* **2011,** *27*, 15312-15321.
21. Liu, C.; Han, X.; Xie, S.; Kuang, Q.; Wang, X.; Jin, M.; Xie, Z.; Zheng, L., Enhancing the Photocatalytic Activity of Anatase TiO_2 by Improving the Specific Facet-Induced Spontaneous Separation of Photogenerated Electrons and Holes. *Chemistry, an Asian journal* **2013,** *8*, 282-289.
22. (a) Ding, X. J.; An, T. C.; Li, G. Y.; Zhang, S. Q.; Chen, J. X.; Yuan, J. M.; Zhao, H. J.; Chen, H.; Sheng, G. Y.; Fu, J. M.,

Preparation and Characterization of Hydrophobic TiO_2 Pillared Clay: The Effect of Acid Hydrolysis Catalyst and Doped Pt Amount on Photocatalytic Activity. *J Colloid Interf Sci* **2008,** *320*, 501-507; (b) Sadeghi, M.; Liu, W.; Zhang, T. G.; Stavropoulos, P.; Levy, B., Role of Photoinduced Charge Carrier Separation Distance in Heterogeneous Photocatalysis: Oxidative Degradation of CH_3OH Vapor in Contact with Pt/TiO_2 and Cofumed TiO_2-Fe_2O_3. *J Phys Chem-Us* **1996,** *100*, 19466-19474; (c) Riassetto, D.; Holtzinger, C.; Langlet, M., Influence of Platinum Nano-Particles on the Photocatalytic Activity of Sol–Gel Derived TiO_2 Films. *Journal of Materials Science* **2009,** *44*, 2637-2646; (d) Pepin, P. A.; Lee, J. D.; Foucher, A. C.; Murray, C. B.; Stach, E. A.; Vohs, J. M., The Influence of Surface Platinum Deposits on the Photocatalytic Activity of Anatase TiO_2 Nanocrystals. *The Journal of Physical Chemistry C* **2019,** *123*, 10477-10486.

23. Monllor-Satoca, D.; Gomez, R., Electrochemical Method for Studying the Kinetics of Electron Recombination and Transfer Reactions in Heterogeneous Photocatalysis: The effect of fluorination on TiO_2 nanoporous layers. *J Phys Chem C* **2008,** *112*, 139-147.

TABLE OF CONTENTS